Remote Sensing Applications: Society and Environment 24 (2021) 100629

Contents lists available at ScienceDirect

Remote Sensing Applications: Society and Environment

journal homepage: www.elsevier.com/locate/rsase

Multi-temporal landslide activity investigation by spaceborne SAR interferometry: The case study of the Polish Carpathians

Kamila Pawluszek-Filipiak [a,*], Andrzej Borkowski [a,1], Mahdi Motagh [b,c]

[a] Institute of Geodesy and Geoinformatics, Wroclaw University of Environmental and Life Sciences, Wroclaw, Poland
[b] Institute of Photogrammetry and Geoinformation, Leibniz University Hannover, Hannover, Germany
[c] Helmholtz Center Potsdam, GFZ German Research Center for Geosciences, Potsdam, Germany

ARTICLE INFO

Keywords:
Landslide activity
Landslide intensity
Persistent scatterers
Interferometry

ABSTRACT

The main goal of this research is to verify the activity state of landslides provided by an existing landslide inventory map using Persistent Scatterers (PS) Interferometry (PSInSAR). The study was conducted in the Małopolskie municipality, a rural setting with sparse urbanization in the Polish Flysch Carpathians. PSInSAR has been applied using Synthetic Aperture Radar (SAR) data from ALOS PALSAR and Sentinel 1A/B with different acquisition geometries (ascending and descending orbit) to increase PS coverage and mitigate the geometric effects due to layover and shadowing. The Line-Of-Sight PSInSAR measurements were projected to the steepest slope, which allowed to homogenize the results from diverse acquisition modes and to compare the displacement velocities with different slope orientations. Additionally, landslide intensity (motion rate) and expected damage maps were generated and verified during field investigations. A high correlation between PSInSAR results and in-situ damage observations was confirmed. The activity state and landslide-related expected damage maps have been confirmed for 43 out of a total of 50 landslides investigated in the field. The short temporal baseline provided by both Sentinel satellites (1A/B data) increases the PS density significantly. The study substantiates the usefulness of SAR based landslide activity monitoring for land use and land development, even in rural areas.

1. Introduction

Landslide Inventory Maps (LIMs) are created using consolidated (field mapping or visual interpretation of stereoscopic aerial photographs) and innovative (remote sensing) techniques (Guzzetti et al., 2012). In the last few decades, differential synthetic aperature radar (SAR) interferometry (DInSAR) has captured considerable attention in the landslide community by offering great support for landslide detection and monitoring (Wasowski and Bovenga, 2014). Nowadays, abundant interferometric synthetic aperture radar (InSAR) applications for landslide studies can be found, e.g., for landslide detection (Meisina et al., 2008; Notti et al., 2010; Bianchini et al., 2012; Motagh et al., 2013; Shi et al., 2020), landslide characterization (Rosi et al., 2018, Zhou et al., 2020; Reyes-Carmona et al., 2020; Shi et al., 2020), landslide monitoring (Notti et al., 2010; Meisina et al., 2008; Haghshenas Haghighi and Motagh, 2016; Herrera et al., 2013; Shi et al., 2020), and landslide activity assessment (Righini et al., 2012; Cigna et al., 2013; Bianchini et al., 2013; Rosi et al., 2018; Reyes-Carmona et al., 2020). This is mainly because SAR missions provide valuable information about ground displacement for a wide area of coverage with a high spatial resolution and great temporal sampling (Bianchini et al., 2013). Multi-temporal interferometric techniques (MTInSAR) have been developed to overcome some DInSAR limitations. Among them, a group of Persistent Scatterer Interferometric (PSI) methods exists, which were firstly introduced by Ferretti et al. (2001), with their approach usually abbreviated in the literature to PSInSAR (Ferretti et al., 2001) and developed further by other scientists (e.g., STAMPS – Hooper et al., 2004; Kampes 2006). MTInSAR methods such as Small BAseline Subset (SBAS) which utilize Distributed Scatterers (DS) and minimize the temporal baseline between SAR images (Berardino et al., 2002; Crosseto et al., 2008) or the SqueeSAR-method which incorporates both DS and Persistent Scatterers (PS) (Ferretti et al., 2011) were also introduced. A wider overview of MTInSAR techniques is provided in Sousa et al. (2011) and Crosetto et al. (2016).

In recent decades, methods for updating landslide inventory maps by exploiting MTInSAR techniques have been utilized by the scientific

* Corresponding author.
E-mail addresses: kamila.pawluszek-filipiak@upwr.edu.pl (K. Pawluszek-Filipiak), motagh@gfz-potsdam.de (M. Motagh).
[1] This paper is dedicated to the memory of Professor Andrzej Borkowski who passed away on March 13, 2021.

https://doi.org/10.1016/j.rsase.2021.100629
Received 22 March 2021; Received in revised form 10 September 2021; Accepted 14 September 2021
Available online 24 September 2021

community. These methods apply traditional thematic maps (geological, topographical, and/or optical images) together with field reconnaissance coupled with InSAR-delivered ground deformation estimates. PSI techniques are mostly used for: (1) landslide phenomena identification (Bianchini et al., 2013; Monserrat et al., 2016); (2) landslide boundary verification or modification (Bianchini et al., 2013; Reyes-Carmona et al., 2020); (3) landslide velocity and intensity estimation (Bianchini et al., 2012); and (4) activity state assessment (Bianchini et al., 2012, 2013; Cascini et al., 2013; Del Ventisette et al., 2014; Kalia, 2018). The commonly used methodology in the abovementioned papers applies the PSI matrix approach with diverse SAR sensors such as Envisat (Cascini et al., 2012; Del Ventisette et al., 2014), ALOS-PALSAR (Bianchini et al., 2013), and more recently, Sentinel −1 (Monserrat et al., 2016 and Barra et al., 2016; Béjar-Pizarro et al., 2017; Kalia, 2018, Bonì et al., 2020; Aslan et al., 2020; Reyes-Carmona et al., 2020; Meng et al., 2020.) A detailed description of the PSI-based matrix approach is presented in Cigna et al. (2013).

In comparison with previous investigations, this study is an extensive and comprehensive exploitation of Sentinel-1A/B images for landslide activity investigation and the first study of such applications in the Polish Carpathians. Particularly, the study area is situated in the proximity of Rożnów Lake. This mostly rural area is also attractive for local tourism. Despite landslide hazards, there is pressure on land development and urbanization (Kroh, 2017). The verification of the objectives and achieved results was conducted through field investigations. Landslide activity states for 43 out of a total of 50 landslides were investigated. Some examples of landslide activity evaluation inspected during the field work are presented. More detailed objectives of this work were to:

- Update landslide activity based on the pre-existing landslide inventory map in the area of Rożnów Lake in Poland from PSInSAR results derived based on ALOS-PALSAR (2007–2010), Sentinel 1A (2014–2016) and Sentinel 1A/B (2017) data;
- Evaluate the effect of SAR geometry delivered by ascending and descending orbits of ALOS PALSAR and Sentinel 1, and the sensitivity of measuring deformation within the study area by using SAR;
- Evaluate the difference in landslide activity updated from three diverse data stacks, namely: L-band (ALOS), C-band with one satellite (Sentinel 1A, with a revisit interval of 12 days), and C-band with two satellites (Sentinel 1A and 1B with a revisit time of six days), respectively;
- Create landslide intensity and expected damage maps based on PSInSAR results.

2. Study area

2.1. Study area and existing landslide database

Landslides are common within the area of the Polish Flysch Carpathians. This constitutes a substantial problem for local communities due to the growing population and the number of properties located within the landslide prone areas (Crozier, 1986). Around 36% of the Polish Flysch Carpathians are affected by landslides (Gorczyca et al., 2013). Therefore, the area with the most active landslides in Poland has been selected for this research. Indeed, the region is known for its frequent landslide occurrence. Within the study area, 501 landslides have been identified over the past years with at least one landslide per 1 km^2. The study area covers a total of 75 km^2, of which 15 km^2 are affected by landslides. Landslides in the study area were mapped for the first time in the 1930s (Gorczyca et al., 2013). Since then, the study area has been affected by mass movements several times, mostly triggered by heavy rainfall. According to historical data, catastrofic landslides activity events have occurred seven times in the study area between 1934 and 1974 (Gorczyca et al., 2013). More recently, in 1997 and 2010, landslides caused catastrophic damage due to abundant rainfall and flooding.

The area of interest is also attractive to tourists. Apart from scattered residential areas, many compact tourist buildings can be found in deforested areas. These areas are characterized by high elevations and drainage divides, which are characteristically affected by landslides. In 2010, catastrophic landslides activity damaged approximately 150 buildings and many roads, transmission lines, crops, and orchards (Gorczyca et al., 2013). According to Gorczyca et al. (2013) and considering the climate change, further catastrophic landslide activity events within the study area are likely, and thus, it is important to monitor all landslide activity in this region.

The study area covers the surrounding hills of Rożnów Lake (Fig. 1). This figure shows the landslide distribution within the study area as well as their predefined activity states. The first preliminary results of PSI applications in the region of Rożnów Lake have been provided by Wojciechowski et al. (2008) and Perski et al. (2010; 2011). Using ERS 1 images, the authors showed the potential of this technique for landslide movement detection in rural and challenging terrains using PSI analysis.

2.1.1. Geological and hydrological settings of the study area

From a geological point of view, the study area is located in the Outer Carpathians of the Magura Nappe, Silesian Nappe, and Grybów Units. These geological units consist of flysch rocks, such as clay, sand, gravel, sandstone, and shale, of the Quaternary and Tertiary periods. The study area is located at the border between the Beskid Wyspowy Mountains and the Carpathian Foothills. Beskid Wyspowy comprises low mountains and middle foothills with slopes ranging from 10° to 35° and elevations from 300 to 340 m. The Magura Nappe is highly susceptible to sliding, especially with respect to hieroglyphic beds containing variegated shales (Burtan et al., 1991; Wójcik et al., 2015). A detailed visualization of diverse geological units is presented in Fig. 2 and the explanation can be found in the supplementary material.

2.1.2. Landslide types and distribution

Diverse landslide types exist within the study area, including translational, rotational, or combined rock-debris slides and typical debris slides (Pawluszek et al., 2018). Many landslides are covered by forest and, therefore, their identification and monitoring present a significant challenge. The landslide activity in the study area is mostly associated with hydro-geological settings such as rock stratification and precipitation. These settingss have created favorable conditions for landslide activation. Catastrophic landslides activity occurred in 2010 due to cumulative rainfall events ranging from 50 to 400 mm over two to five days activating mudslides and debris slides. The activation of deep rockslides required a long continuous precipitation event of 100–500 mm per month. Most of the landslides scarps within the study area lead down to valley floors or river terraces where the colluvium consists of weathering debris, clay debris, and pure clay. Usually, north-facing landslides tend to be complex, while south-facing landslides tend to be insequent or subsequent slides (classification based on the relationship to the arrangement between rock layers as described in Gorczyca et al. (2013)).

2.1.3. Pre-existing landslide inventory map

The Landslide Counteracting System (SOPO) project was used as the preexisting landslide inventory database. LIMs are the components of this database. The SOPO project was launched in 2008 under the order of the Ministry of Environment with funds from the National Fund for Environmental Protection and Water Management. The purpose of SOPO is to support the administration and environmental protection inspectorates, as well as non-governmental organizations, in effectively fulfilling the duties connected to landslide risk management. The system, in its assumptions, provides proper and complete data for effective landslide risk management (Pawluszek et al., 2018). All recorded landslides locations and their extent have been stored within the SOPO project. Moreover, information about the activity state, as well as

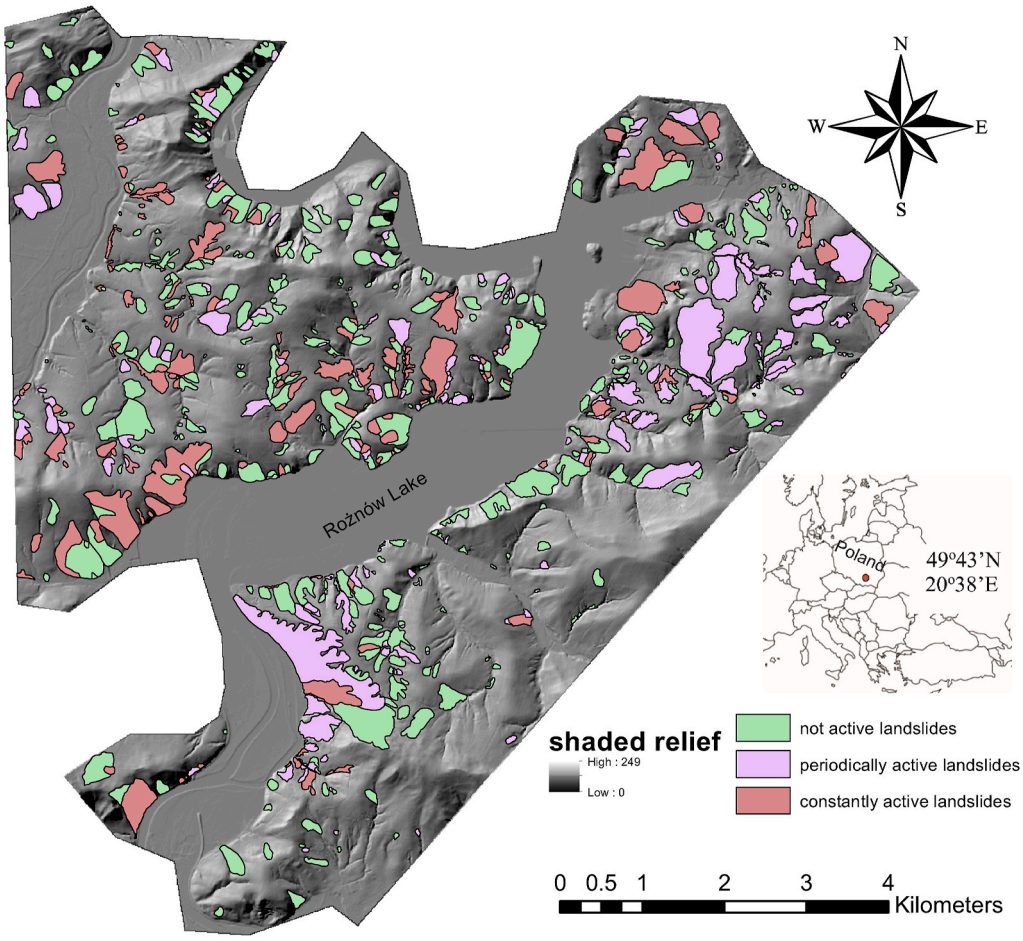

Fig. 1. Location of the study area and landslide distribution with a pre-existing activity state, overlaid on a hillshade map derived from a Digital Elevation Model.

detailed geomorphological and geological analyses, are presented. Landslides within the study area were mapped during field work in 2010, 2011, 2012, 2013, 2014, and 2015 (Bąk et al., 2011; Wójcik et al., 2011; Koluch and Nowicka, 2012). Additional mapping was also performed based on topographic maps at a 1:10,000 scale and supported by stereoscopic analyses of aerial photographs and LiDAR data (Perski et al., 2011; Wojciechowski et al., 2012). A total of 506 landslides were identified in this area. Many of them are complex landslides which were mapped within the SOPO from more than one object. These objects have been distinguished according to the activity state of a specific landslide unit. Therefore, in total, 712 landslide objects exist in the database. These landslides cover 15 km^2 of the study area. This means that 20% of the study area is affected by landslides. According to the preexisting landslide inventory, 50%, 26%, and 24% are considered as not active, periodically, active, and continuously active landslides respectively. Landslides within the study area are translational and rotational landslides; however, the SOPO database does not differentiate translational and rotational slides and these both types are described in general as "slides". Moreover, there are small landslides within the study area, with an area of a few ares (a) and big complex landslides with an area exceeding 5000 ares. The precise number of landslides, their activity and the statistical overview of the area are presented in Table 1 while the spatial distribution is presented in Fig. 1.

2.2. Methods

The methodology flowchart is presented in Fig. 3. The generation of landslide activity maps integrates the SAR data, the PSInSAR post-processed delivered products, and the landslide inventory map. These three consecutive stages are described in the following subsections.

2.2.1. Radar data and PSI processing

Table 2 presents five different data stacks, which have been processed using PSInSAR. To evaluate the benefits of launching an additional Sentinel-1 satellite in terms of PS point density, we split the Sentinel datasets into a stack of Sentinel-1A images covering the period of 2014–2016 and a stack of Sentinel-1A/B images covering the year of 2017. Due to the limitation of traditional DInSAR techniques related to the degradation of radar signals resulting from atmospheric effects and temporal and geometrical decorrelation, the PSInSAR approach has found widespread applications in landslide studies (Perski et al., 2011; Bianchini et al., 2012). The PSInSAR approach is based on the exploration of stable natural or man-made reflectors which present a stable backscattering signal over time. As a matter of fact, the PSInSAR approach has previously been applied for monitoring Carpathian landslides (Perski et al., 2010, 2011). However, due to the high temporal decorrelation resulting from vegetative cover and short wavelengths (X-band), it was only partially successful (Perski et al., 2009; Perski et al. (2011). This is mostly related to the low PS density due to the application of TerraSAR-X data. Therefore, the exploitation of C-band (Sentinel-1) and L-band (ALOS PALSAR) data can present more advantages, especially in rural areas.

In this work, we exploited the PSInSAR approach introduced by Ferretti et al. (2001). This approach utilized more than 20 images to separate diverse interferometric components which correspond to deformation components, atmospheric error, or topographic error due to the differences between digital terrain modelling (DTM) used for topography estimation and determining real surface backscattering

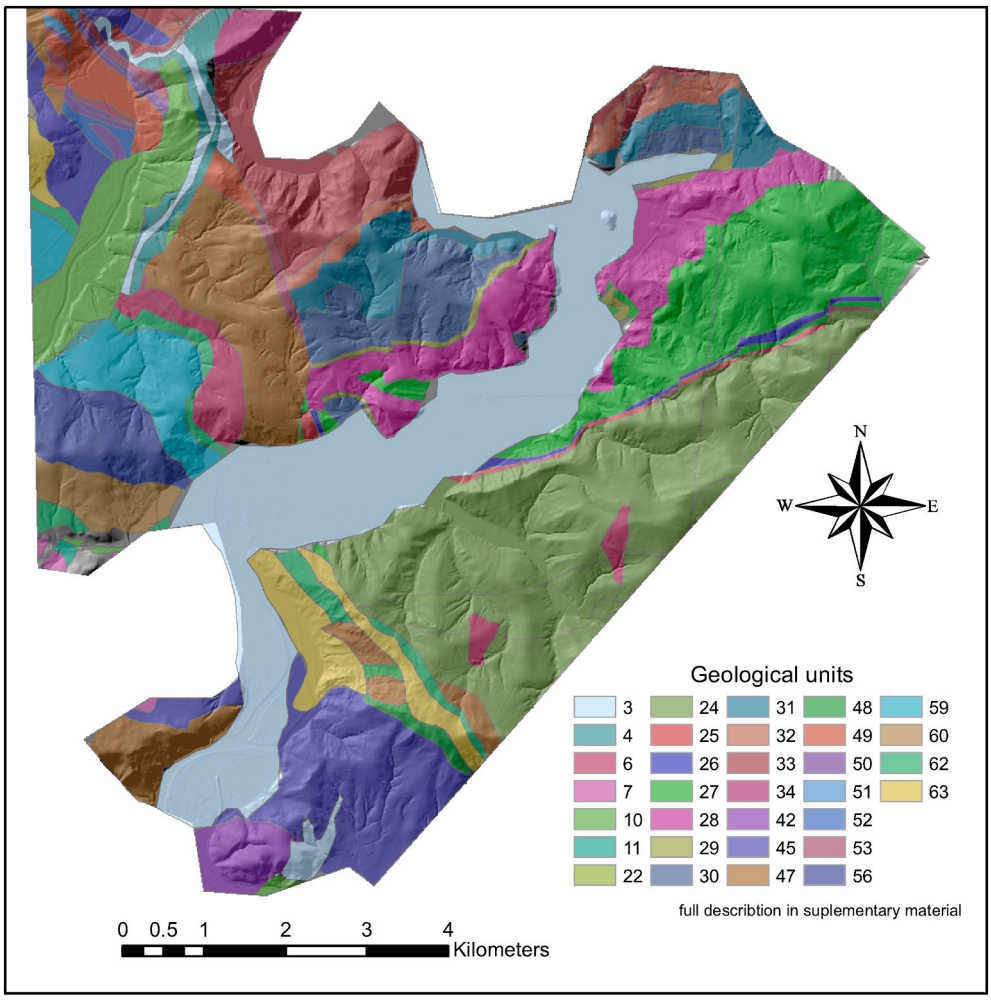

Fig. 2. Geological setting of the study area. The legend of the study area is presented in the supplementary material.

Table 1
Number of landslide within the study area and its sizes.

Activity state	Number of landslide objects	Min area [a]	Maximal area [a]	Mean area [a]
Continuously active	173	11.22	2960.38	249.46
Periodically active	185	6.85	6688.88	242.33
Not active	354	5.46	2536.74	175.83

elevation. The PSInSAR approach is based on the following steps: (1) interferogram generation with respect to a common master image; (2) PS candidate selection based on amplitude dispersion index; (3) first estimation of atmospheric phase screen (atmospheric influence) and topographical and displacement components; and (4) second estimation of interferometric components and final PS points selection. For a precise description of the algorithms applied within each step, see Ferretti et al. (2000; 2001).

The presented approach was performed for ALOS and Sentinel data stacks independently. Some necessary preprocessing steps were applied for raw SAR data, namely, focusing, image cropping, and compensating for the zero Doppler centroid. SARscape® software was used for SAR data processing (Sahraoui et al., 2006). During the co-registration step, all images were co-registered onto the resampled Master file image. This involves an oversampling of a factor 4 and 2 in range direction for ALOS PALSAR and Sentinel-1 data, respectively. This parameter was utilized to avoid aliasing of fast fringes in the case of large baseline values. Since the PSInSAR approach looks at point targets, the spectral shift and the common Doppler bandwidth filters are not executed. The interferograms are then generated for each slave image always using the same master image. The precise orbital files from the European Space Agency (ESA) were used. The 3-arcsec SRTM DTM (resolution approx. 90 m) was applied for topographic phase removal and geocoding. Amplitude dispersion index of 0.25 was utilized as a threshold for PS candidate selection, and the final PSs were extracted with a coherence value higher than 0.75. Low pass spatial filtering of the Atmospheric Phase Screen (APS) was set as 1200 m and high-pass temporal filtering of the APS was set as 365 days. The same parameters were utilized for PS processing of all five various SAR datasets.

2.2.2. *Persistent scattering (PS) postprocessing*

After PSInSAR processing, all results for the five diverse data sets were post-processed to retrieve the most adequate displacement information (see module 2 in Fig. 3). PSInSAR measurements provide deformation information on the LOS direction (from the satellite to the ground as determined by the incident and heading angles). Thus, it is impossible to retrieve the 3D displacement from InSAR directly. The horizontal and vertical components of the movement (assuming no N–S horizontal motion exists within the study area) can be retrieved by combining measurements from ascending and descending orbits. However, in mountainous areas, where PS coverage is low due to geometrical conditions and distortions, velocity decomposition can be problematic. Therefore, the conversion of LOS deformation into the most probable

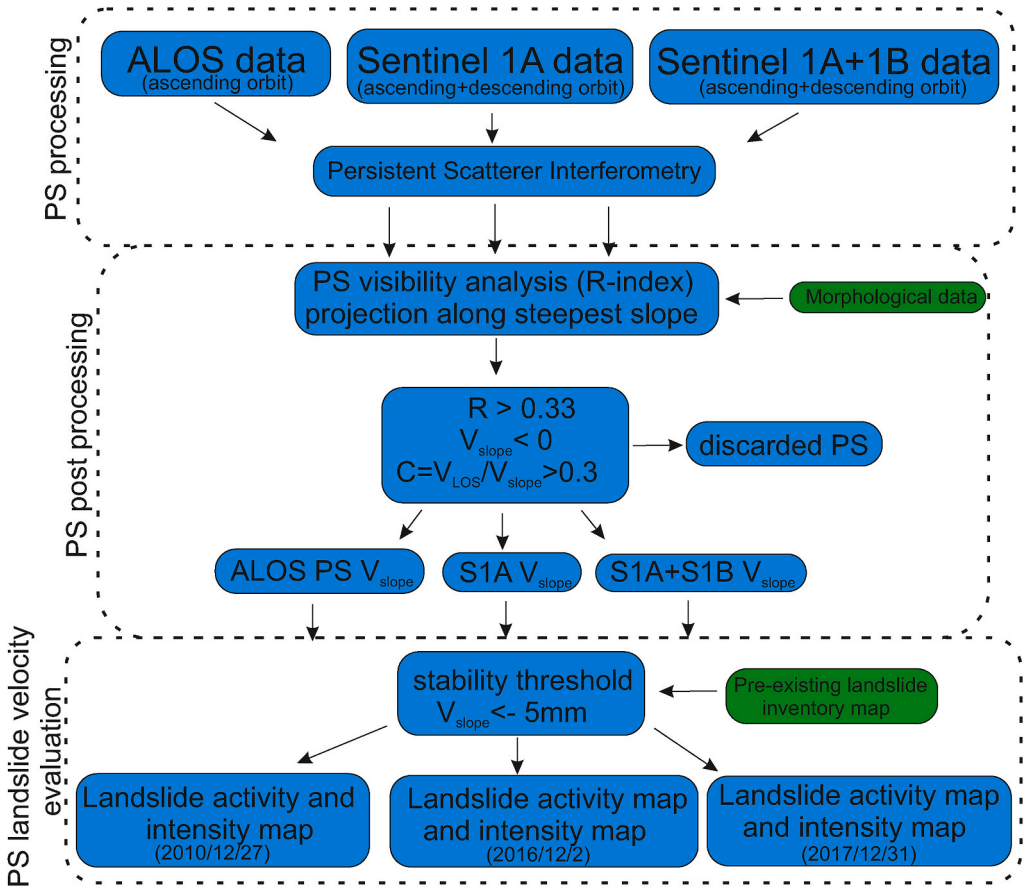

Fig. 3. Methodology.

Table 2
Data stacks used and their metadata.

	Data stack 1	Data stack 2a	Data stack 2b	Data stack 3a	Data stack 3b
Satellite	ALOS PALSAR	Sentinel 1A	Sentinel 1A	Sentinel 1A+1B	Sentinel 1A+1B
Wavelength	L-band	C-band	C-band	C-band	C-band
Repeat cycle [days]	46	12	12	6	6
No. of images	22	56	52	60	53
Orbit mode	ascending	ascending	descending	ascending	descending
Spanning interval	31/01/ 2008-27/ 12/2010	29/11/ 2014-24/ 12/2016	8/12/ 2014-21/ 12/2016	5/01/ 2017-31/ 12/2017	2/01/ 2017-22/ 12/2017
Polarization	VV	VV	VV	VV	VV
Incidence angle	38.7	39.05	33.71	33.04	33.71

direction (direction of maximum slope), by assuming a pure translational movement mechanism, is commonly used (Bianchini et al., 2012). We applied the R index to assess the sensitivity of InSAR LOS measurements at a specific point. This index represents the geometrical visibility of the specific area with respect to the SAR system used. The R index considers the morphology of the study area and the acquisition geometry of the SAR system and is calculated as presented in Notti et al. (2010):

$$R = -\sin(S \cdot \sin(A - \alpha + 90) - \vartheta) \quad (1)$$

where α is the angle of the satellite track from north, ϑ is the incidence angle, S is the slope, and A stands for the aspect. The calculated R index can take values within the range of [-1, +1]. Fig. 4 provides the visualization of the R values over the study area for ALOS and Sentinel imaging systems.

An R index close to zero shows the low sensitivity of SAR to measured displacements for specific locations. Based on experiments for different test sites, Notti et al. (2014) discovered that distinguishing four classes is the optimal solution. Therefore, the R index has been divided into four classes, wherein we used the same interval length for all classes except the first. The first class (R index <0) represents the locations where the detection of PS points is difficult due to geometrical distortions. The second class (R index 0 to +0.33) indicates the locations where the slope geometry is not convenient for SAR measurements. The third group (R index 0.33 to 0.66) represents areas where PS occur on slopes with an acceptable geometry for SAR displacement measurements. The fourth group (R index 0.66 up to 1) represents the high sensitivity of LOS deformation monitoring. This means that, in this location, the slope direction is almost parallel to the satellite LOS direction and SAR sensors can perfectly measure the deformation over this location. In summary, in further steps, the PS points with an R index higher than 0.33 were considered.

Deformation retrieved from PSInSAR is a 1D measurement in the direction of the satellite. LOS deformations (V_{LOS}) were projected along the steepest slope according to the equation:

$$V_{slope} = V_{LOS}/\cos\beta \quad (2)$$

with β as the angle between the steepest slope and the LOS direction.

Despite the great advantage of the motion represented in the slope direction, this projection has some limitations. First, when $\beta = 90°$, V_{LOS} goes into infinity and V_{slope} is exaggerated. Here, we followed Herrera et al. (2013) and selected an absolute maximum value of $\beta = 72°$, which is equivalent to $\cos\beta = 0.3$. Thus V_{slope} cannot be higher than 3.33 times

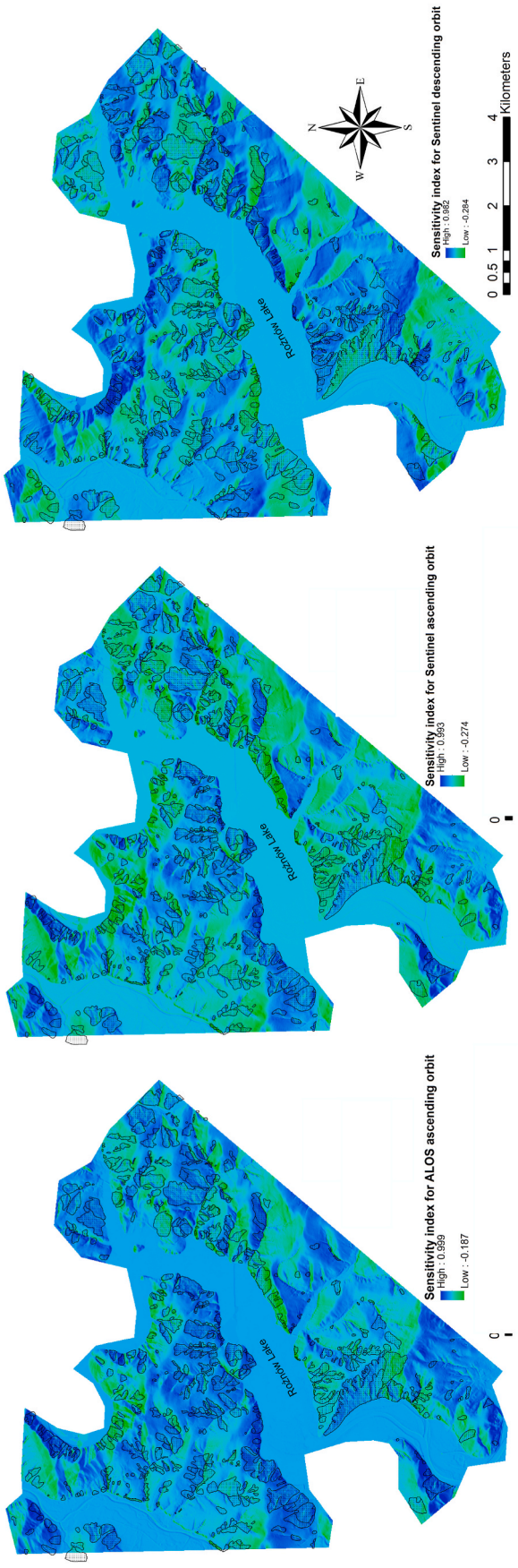

Fig. 4. R index for three diverse satellite geometries (ALOS in ascending and Sentinel in ascending and descending modes).

V_{LOS}. To remove any V_{slope} exaggeration, we considered only the PS points for which cosβ >0.3.

Moreover, we discarded PS points which showed V_{slope}>0 because positives values represent uphill movements and it is not representative for small landslide movements, even though positive values exist within landslides, especially in the toe area.

2.2.3. *Velocity thresholding for activity state estimation - PSI based matrix approach*

For the activity and intensity assessment, some representative values were retrieved from PSI analysis. These values are fixed values which are used for: (1) distinguishing between moving and non-moving landslides, and (2) discriminating between extremely slow from very slow-moving landslides. It strictly depends on the study site considering the deformation processes and typology (Cigna et al., 2013). Commonly, the average of velocity estimates is applied as a representative of velocity (Bianchini et al., 2012). However, different thresholds are applied to assess the landslide activity. These values can vary with respect to SAR data wavelength and the projection of the velocity. For V_{LOS}, some authors (Righini et al., 2012; Herrera et al., 2013) utilized 2 mm/yr as the velocity threshold for landslide activity assessment for C-band data and 5 mm/yr for V_{slope} (Cigna et al., 2013; Bianchini et al., 2013). These changes are mostly correlated with different velocity distribution patterns. For the LOS velocity, the distribution is almost normal (Gaussian), while for SLOPE it is negatively skewed as a result of the PS reduction (Bianchini et al., 2013). Therefore, for activity state estimation, we applied 5 mm/yr as the V_{slope} threshold. Based on the preexisting landslide inventory map and PSInSAR post-processed results, we applied the PSI-based matrix approach (Fig. 5). According to the PSI matrix (Fig. 5), the presented approach employs a simplified version of the official categorization of the landslide activity state presented in the landslide glossary WP/WLI (1993). Four diverse activity states were determined (Fig. 5): (1) reactivated = active after being inactive, (2) active continuous = currently moving, (3) dormant = inactive, but possible to be reactivated, and (4) stabilized = not active anymore.

2.2.4. *Landslide intensity estimation*

Based on the representative values of deformation, landslide intensity was assessed relying on the Cruden and Varnes (1996) intensity scale. This scale is based on PSI velocities consisting of three categories: negligible, extremely slow, and very slow (Fig. 6). Regarding Cruden and Varnes (1996), landslides with sufficient information are divided into negligible (mean velocity 5 mm/yr), extremely slow (mean velocity between 5 and 16 mm/yr), and very slow (mean velocity between 16 mm/year and 1.6 m/yr). It is also worth mentioning that some researchers use slightly lower thresholding (e.g., Bianchini et al., 2012) with the argumentation that PSI underestimates movements in comparison to real movements.

3. Results

3.1. *Landslide activity state and intensity map generation*

The landslide activity and intensity maps integrate the post-processing derived products (R and V_{slope}) with the existing landslide inventory. For the assessment of landslides activity, the previously described PSI matrix-based approach was applied. Results of the activity assessment are presented in Fig. 7. However, the activity state was presented only for landslides where sufficient PS points were found. At least four PS points within a landslide body were set up as the threshold. Several landslides in the study area are complex landslides. Such landslides are divided into parts and represented in SOPO databases as separate objects. In this case, the mentioned threshold is related to each landslide object.

In Fig. 8, the landslide intensity scale was estimated based on the

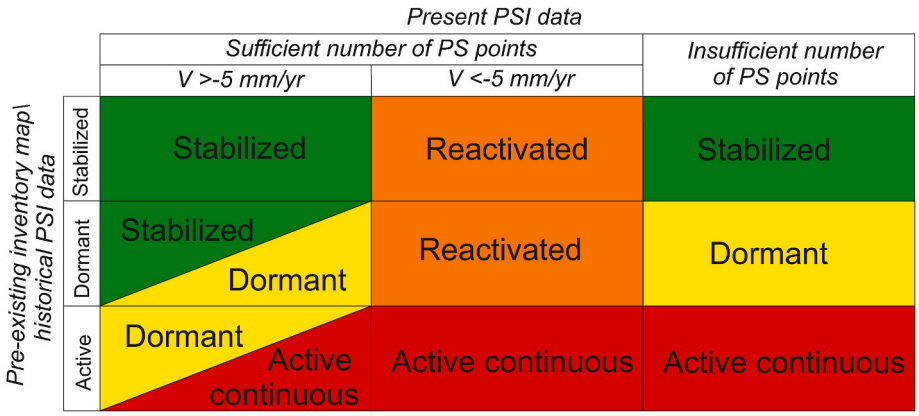

Fig. 5. PSI based matrix activity assessment (based on Cigna et al., 2013).

Present or historical PSI data			
sufficient number of PS points			insufficient number of PS points
Vp or Vh>- 2mm	-2mm<Vp or Vh<-10mm	Vp or Vh <-10mm	
neglible	extremely slow	very slow	NC

Fig. 6. Classification of PSI delivered movement rates for landslide intensity scale estimation. V_p and V_h are present or historical PSI estimated movements, respectively.

abovementioned classification (subsection 2.2.4).

After the postprocessing phase, 3898, 5260, and 10,798 PS points were found within the landslide boundaries for ALOS PALSAR, Sentinel 1A, and Sentinel 1A/B data stacks, respectively. This allowed us to estimate the activity state and intensity scale for 128, 130, and 205 landslides using ALOS, Sentinel 1A, and Sentinel 1A/B data, respectively.

Fig. 9 presents some statistics of landslide activity state assessment depicted in Fig. 7 in the form of pie charts. The left column of the pie charts in Fig. 9 corresponds to the maps shown in Fig. 7 (a), (c), and (e) respectively. From the total number of landslide and landslides objects (according to the SOPO database), 23%, 20%, and 38% have been updated by the PSInSAR approach for ALOS, Sentinel-1A, and Sentinel-1A/B data, respectively. The percentages of particular activity states within the updated landslides are illustrated in the right column of the pie charts in Fig. 9. These pie charts correspond to the maps in Fig. 7 (b), (d), and (f). Note that the last maps show activity states updated based on the PSI matrix. Therefore, there are also landslides, whose activity states have been updated based on historical or preexisting data (SOPO database) if an insufficient number of PS were detected on the landslide object (compare with Fig. 5).

3.2. Possible damage assessment

Based on a literature review, a downstream investigation was performed, and additional thresholds were set up to assess the possible damage related to buildings and infrastructures located in landslide areas. For this purpose, we applied the method proposed by Mansour et al. (2011), i.e., a threshold of 10–100 mm/yr as a minimum landslide velocity which can cause moderate damage to infrastructures and buildings. Velocity rates greater than 100 mm/yr can cause major damage to infrastructures and buildings. Landslides with velocities below 10 mm were classified as landslides with minor expected damage. This thresholding was adopted as an additional criterion to support environmental planning and management strategies in areas which can be characterized by high landslide hazard and, consequently, should be addressed with potential damage protection. In Fig. 10, possible damages caused by mass movements in the study area are presented for three diverse PSInSAR processing results.

3.3. Field validation

The confidence degree of landslide activity maps can be validated throughout their comparison with external independent sources, such as damage inventories, in situ measurements, field checks, etc. This evaluation aims to assess whether the measured displacements represent landslide dynamics. It is worth emphasizing that the reality of the PSInSAR velocity estimation itself is not assessed due to the lack of external field measurements, but this measurement may be related to landslide activity. For this reason, field verification was performed.

Due to the abundant number of landslides located within the study area (506), only 50 landslides, which are expected to produce moderate damage, were investigated in the field. Activity states were confirmed for 43 landslides, which indicates a success rate of about 86%. However, even if no evidence was found in the field, it does not mean that the landslide is not active. Landslide damage, especially in agricultural areas and on buildings, are immediately repaired and, therefore, not always visible to people living there. Some examples of field verification and descriptions of the investigated landslides are presented in the following subsection. The field work was performed in November 2018 and was led by an experienced landslide expert.

3.3.1. The "Just-Tęgoborze" landslide (SOPO ID 23374)

The "Just-Tęgoborze" landslide is a group of rock and debris slides occurring below St. Just pass. This landslide is located on the southern and eastern slopes. The landslide was developed on clay of various genesis and from the marginal Magura Nappe formation. The upper part is founded on the outcrops of the Magura sandstones and the lower part on the slate sandstones of the sub-Magura unit. It has been documented as being active for the past 50 years. Its activity state is regularly confirmed by road damage. Essential movements occurred in June 2010 due to abundant rainfall. In addition, many residential buildings were

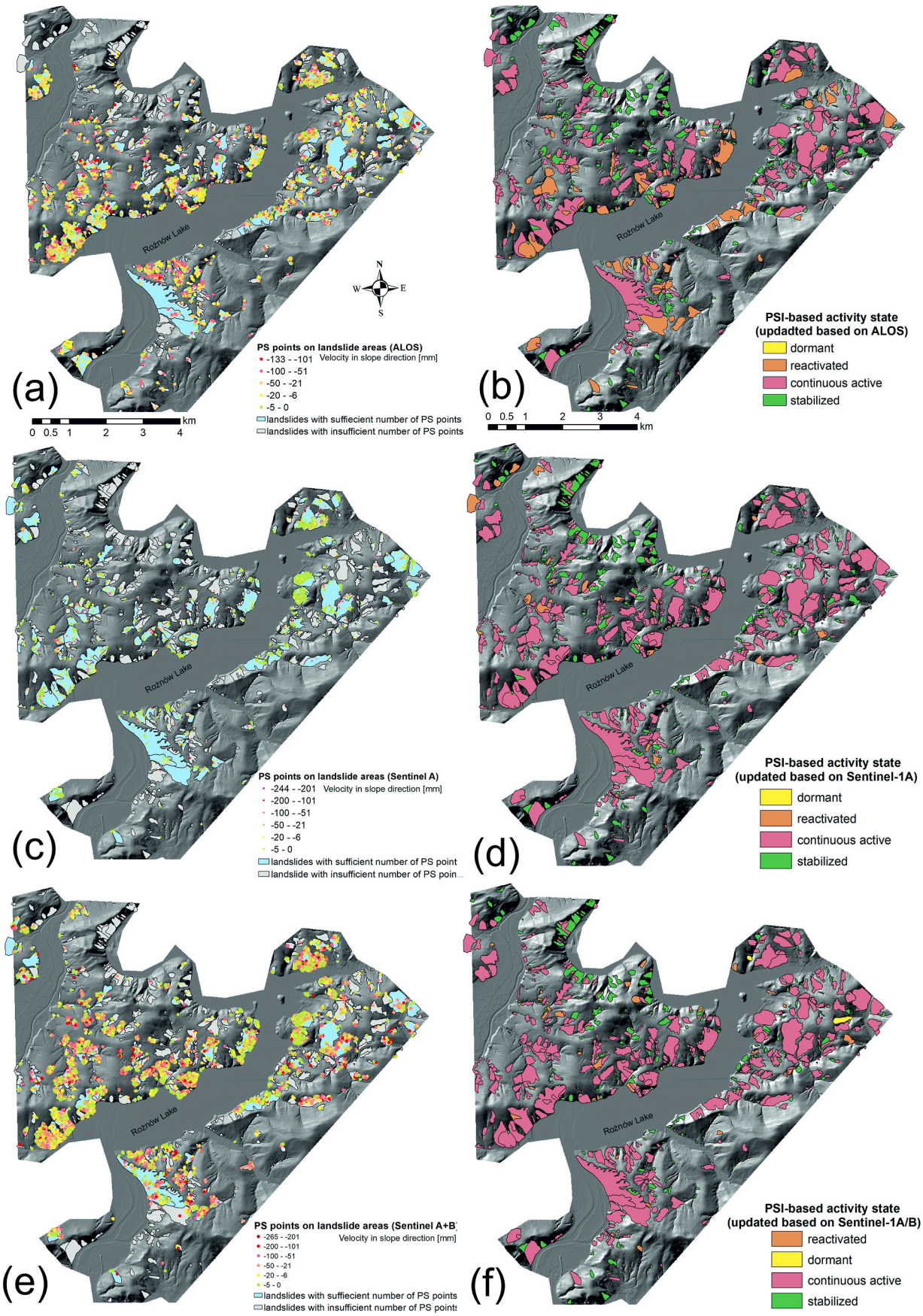

Fig. 7. PS points after post-processing phase (on the left) and landslide activity state assessment (on the right) based on PSI analyis of three data stacks.

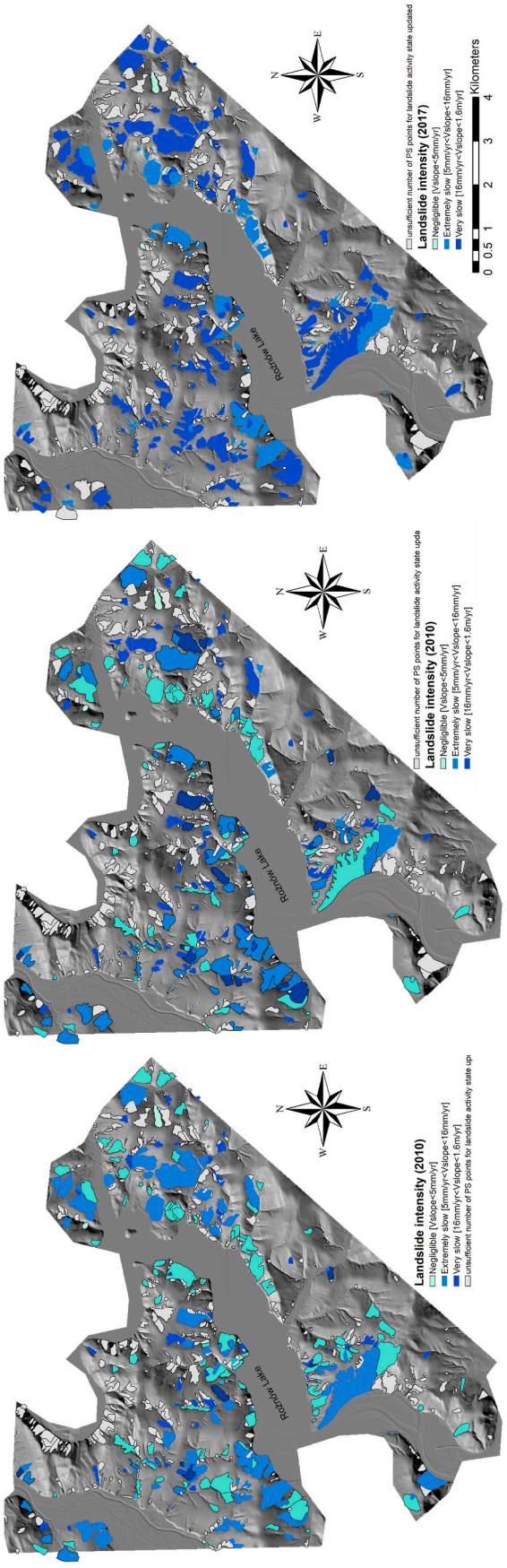

Fig. 8. Landslide intensity scale estimation based on ALOS, Sentinel 1A, and Sentinel 1A/B PSI results.

damaged. Landslides tend to develop and increase in activity over a large area. The presented landslide is very difficult to stabilize due to their activity, the considerable thickness of the colluvium, and the presence of slate shales in the ground (Wójcik et al., 2011). This landslide was assessed as active (in 2010), dormant (2014–2016), and reactivated (in 2017) based on the PSI-based matrix approach. Within the landslide area, there were moderate damages in 2010 and 2017, and minor damages in 2016 according to Mansour et al. (2011). In Fig. 11, the extent of the Just-Tęgoborze landslide and PS points are presented together with photographs taken during the field verification.

3.3.2. The "Zbyszyce" landslide (SOPO ID 73253)

The Zbyszyce landslide is situated in the Zbyszyce village in the Gródek nad Dunajcem commune on the northwestern slope of the Dąbrowska hill (581 m above sea level). It covers the whole slope up to the bottom of the Dunajec River Valley, where the river forms a delta. The landslide is located in the overlapping area of Magura and Dukla Nappes. The Magura units occupy the largest area under colluvial sediments and are represented by thin and medium-sized dominant sandstones and clay and mud shale layers of larchwort belonging to Stratiflycam (Santon-Paleocene). Above them, in the dorsal part, there are speckled slates overfilled with thin sandstones (Paleocene-Eocene). In the south and southeastern directions, these settlements are also flat on the pieces which belong to the Dukla unit. In the southern part of the landslide, there are thick-walled Cergowa sandstones (from Oligocene) and in the eastern part sandstones and shales of the Lower Krosno layers (Perski and Wójcik, 2010a; Wojciechowski et al., 2012).

In addition to the discontinuities associated with the slides, the geological structure of the landslide is marked by faults. The Zbyszyce landslide has been active for at least 60 years. The communal road crossing is constantly being destroyed by the landslide in its middle and lower parts. This landslide was assessed as active (in 2010), dormant (2014–2016), and reactivated (in 2017) based on the PSI-based matrix approach. Within the landslide area, there were expected moderate damages (in 2010 and 2017) and minor damages (in 2016). The extent of the Zbyszyce landslide and PS points are presented in Fig. 12, together with photographs taken during the field verification and documentation of active landslide conditions.

3.3.3. The "Lipie-Jelna" landslide (SOPO ID 73194)

The "Lipie-Jelna" landslide is located between the towns of Lipie and Jelna. The landslide is a rock and debris slide. The landslide material consists of clays, sandstones, and shales from the Quaternary period. It is an old landslide with main scarps located more or less parallel to the extent of the landslide, ending with a 3 m landslide crown. The landslide area covers the whole area of the slope. When reactivated, this landslide covered about 80% of the landslide area. It tends to develop uphill, and its activity depends on weather conditions. Many building cracks, as well as damage to roads and cultivated fields exist within the area of the landslide (Wójcik and Krawczyk, 2010). This landslide has been assessed as active based on all PSInSAR results with moderate damage caused by landslide activity. The extent of the Lipie-Jelna landslide is presented in Fig. 13, together with photographs taken during the field verification.

3.3.4. The "Wola Kurowska" landslide (SOPO ID 73254)

The Wola Kurowska landslide is located on the eastern slope of the ridge, 418.8 m above sea level and on the eastern part of the provincial road. The landslide is a rock and debris slide consisting of clay, sandstone, and shale that was probably created in the late Holocene. The main scarp of the landslide is heavily obliterated. The landslide is developed in the Magura Nappe and the Silesian Nappe. As a result of continuous rainfall in 2010, 20 m of provincial road and two buildings in agricultural areas were damaged. This landslide had probably been active earlier as well, as indicated by the ruins of older buildings (Perski and Wójcik, 2010b). This landslide was assessed as active (in 2010), dormant (2014–2016), and reactivated (in 2017) based on the PSI

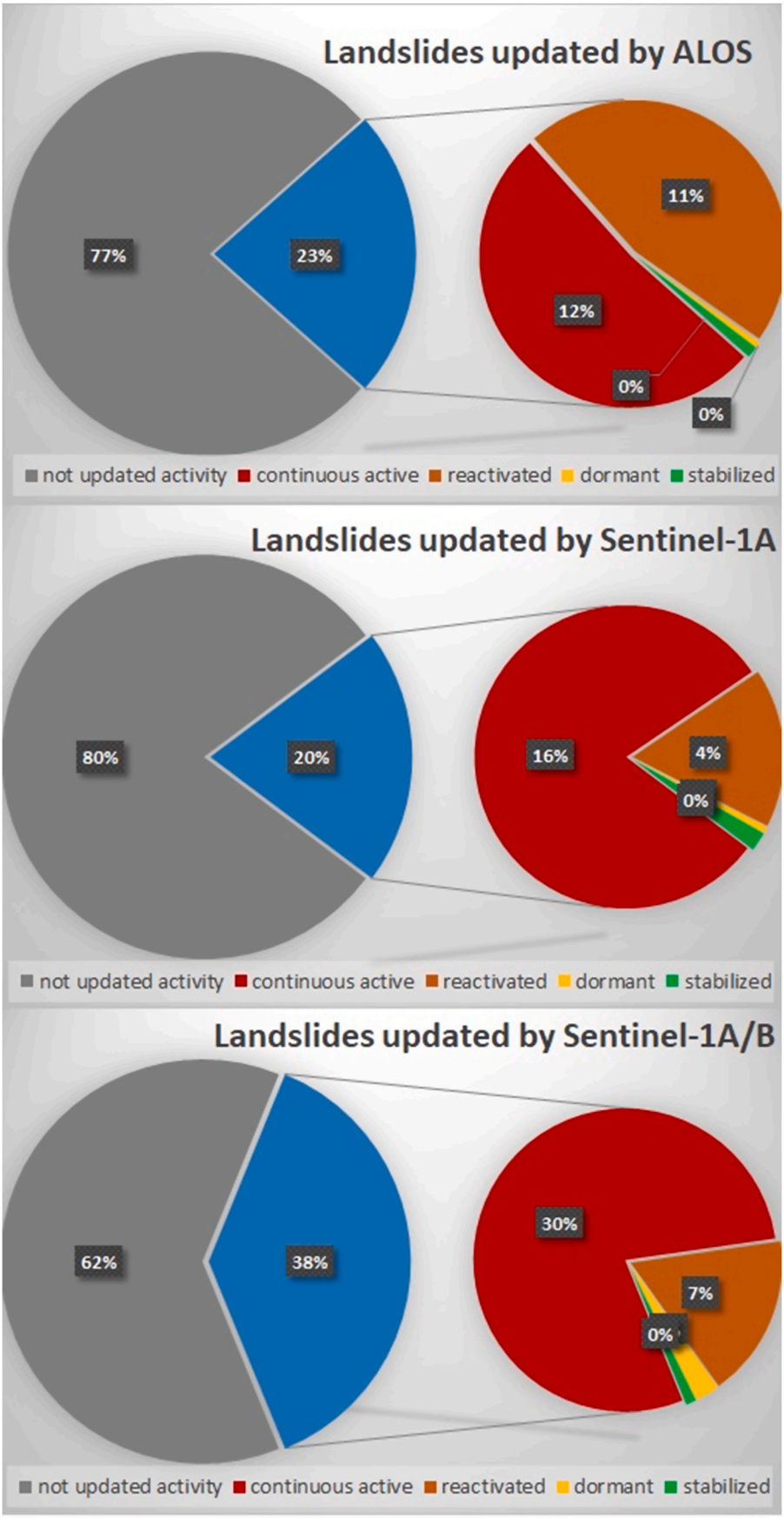

Fig. 9. Percentage of updated landslides.

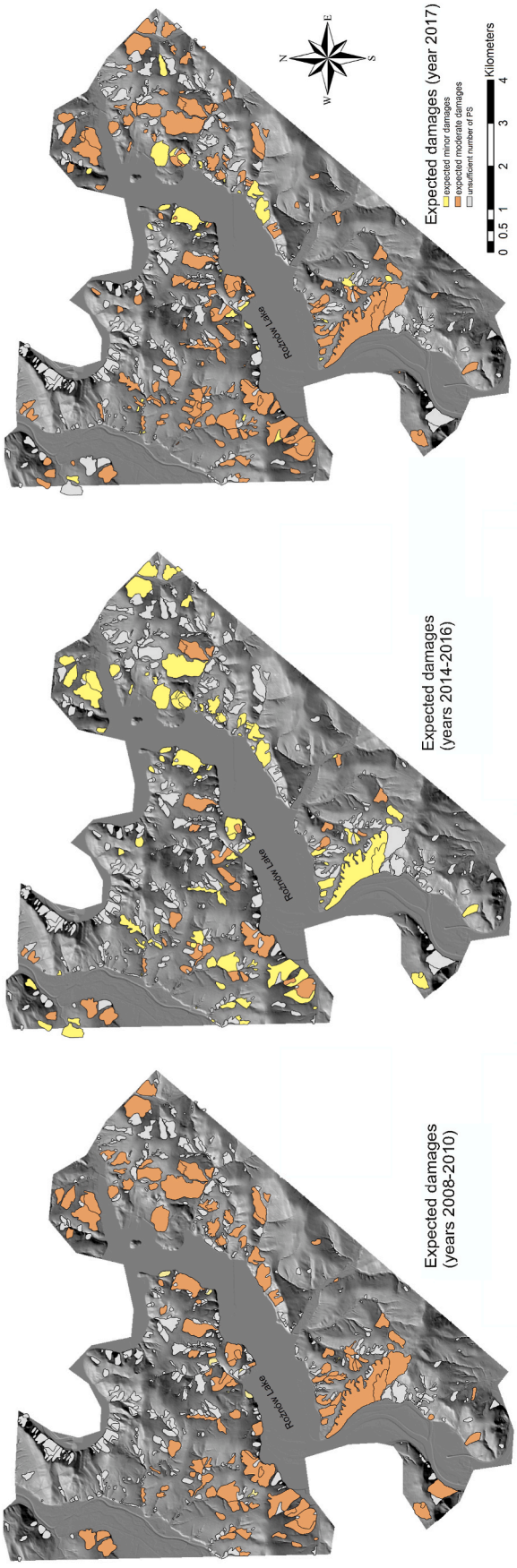

Fig. 10. Expected damage from landslides based on Mansour et al. (2011) and PSI results from ALOS, Sentinel 1A, and Sentinel 1A/B data.

matrix approach. There were expected moderate damages in 2010 and 2017 and minor damages in 2016 due to landslide activity. The extent of the Wola Kurowska landslide is shown in Fig. 14, together with photographs taken during the field verification. There is a clearly visible correlation between the assessed landslide activity and damage observed.

3.3.5. The "Bartkowa-Posadowa" landslide (SOPO ID 72917)

The Bartkowa-Posadowa landslide is a rock and debris slide covering almost all parts of the slope. Its characteristic landslide features are destroyed and transformed by intensive agricultural activity. It is a frontal landslide which means that its width is greater than its length. The main slope has a tendency to develop up the slope which causes damage to the communal road. There are transverse faults and a drop of up to 0.5 m on this road, and the depressions are repaired by leveling the surface. Other communal roads have also been destroyed.

Numerous forms (scarps, cracks) characteristic of active landslides were found during the field check. The landslide is active over almost the whole area. There are more than 20 residential buildings with visible damage to the walls and floors. It is not possible to stabilize the entire landslide, as well as fragments of landslides and current landslide processes, due to the depth of the slip surface (up to 22 m) (Chowaniec et al., 2012). Destroyed buildings are not suitable for renovation, and residents should be resettled. This landslide was assessed as active (in 2010), dormant (2014–2016), and reactivated (in 2017) based on the PSI-based matrix approach. There were moderate damages in 2010 and 2017 and minor damages in 2016 according to Mansour et al. (2011). The extent of Bartkowa-Posadowa landslide is visualized in Fig. 15, together with photographs taken during the field verification.

4. Discussion

The outcomes of the conducted investigations confirmed the utility of the PSI technique in the field of landslide activity and intensity assessment. Moreover, PSInSAR results can be applied in security management for assessing potential hazards related to the occurrence of landslides. However, PSI application needs to be carefully evaluated. Even if the use of the PSI technique can overcome some of the limitations of conventional monitoring techniques (e.g., large coverage of the area to be monitored, high costs, terrain inaccessibility, installation problems, and maintenance), in many cases, the assessment of landslide activity might become very challenging. This is mostly due to PS density in rural areas, where temporal decorrelation affects PS density. However, it was demonstrated that increasing the temporal sampling rate in view of launching the second Sentinel 1 satellite provides a higher PS density and, ipso facto, more landslides could be investigated by means of PSInSAR. We were able to investigate the landslide activity states of 130 and 205 landslides by using one Sentinel satellite and two satellites, respectively. This represents significant progress in comparison with the first attempts with the application of the PSI technique using TerraSAR-X and ERS-1 data in this study area (Perski et al., 2010, 2011) which were unsuccessful due to disturbing vegetation cover.

From another point of view, the application of two Sentinel datasets from ascending and descending orbits using only one Sentinel satellite (C-band) allowed us to achieve a similar PS density in comparison to the one ascending dataset of ALOS PALSAR (L-band). For both sensors, ALOS and Sentinel 1 in ascending geometry, the slope movement in a NE-SW direction represents only a small percentage of the real occurred displacements in LOS displacement rates measured with the interferometric analysis. This means that many landslides which are facing mostly northeast or southwest slopes cannot be monitored using interferometry with ascending acquisition geometry. For these slopes, the descending geometry is more suitable, and thus, deformation monitoring from both acquisition modes should be combined. Therefore, the projection of the V_{LOS} along the steepest slope permits us to homogenize the landslide velocity achieved from PSInSAR processing from diverse

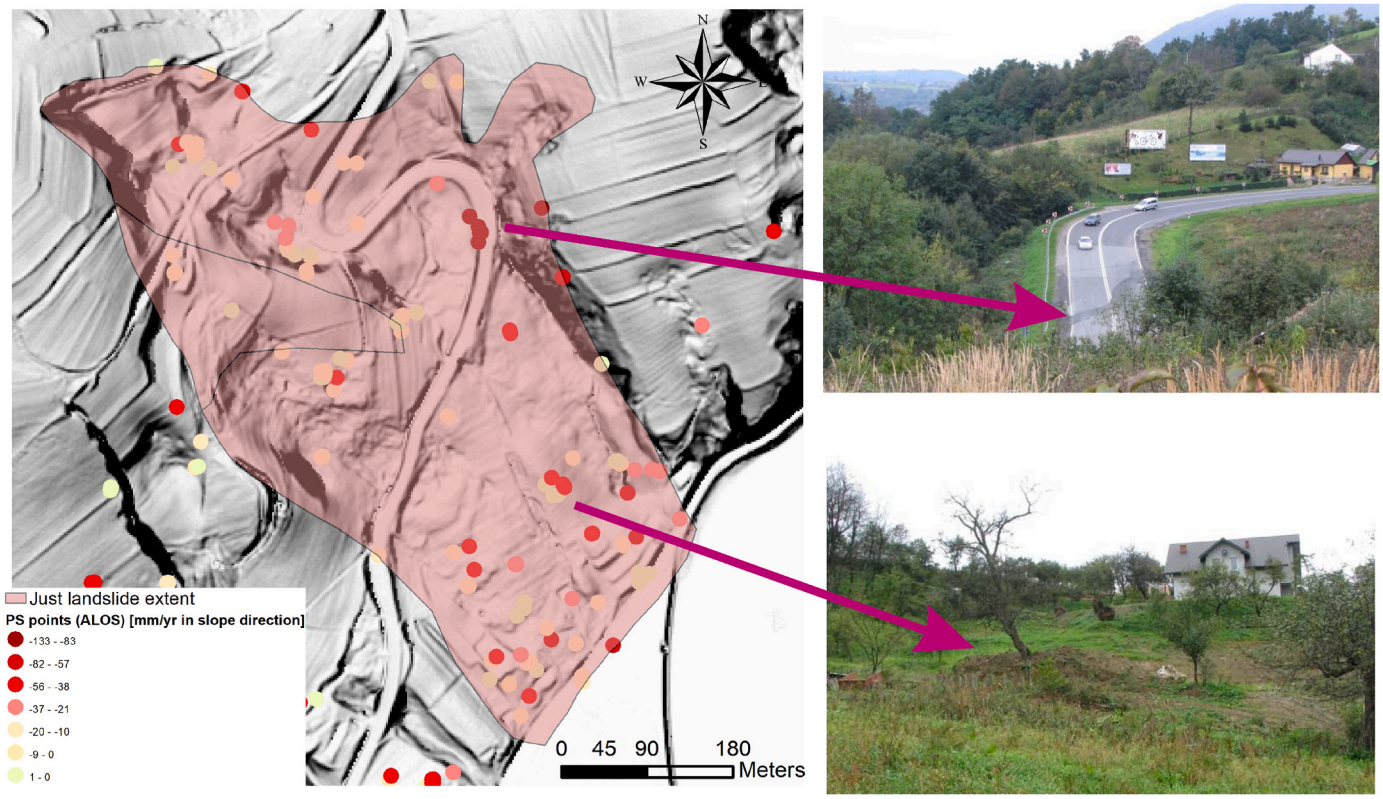

Fig. 11. Just-Tęgoborze landslide activity evaluation during field trip (photo taken on 9/29/2010).

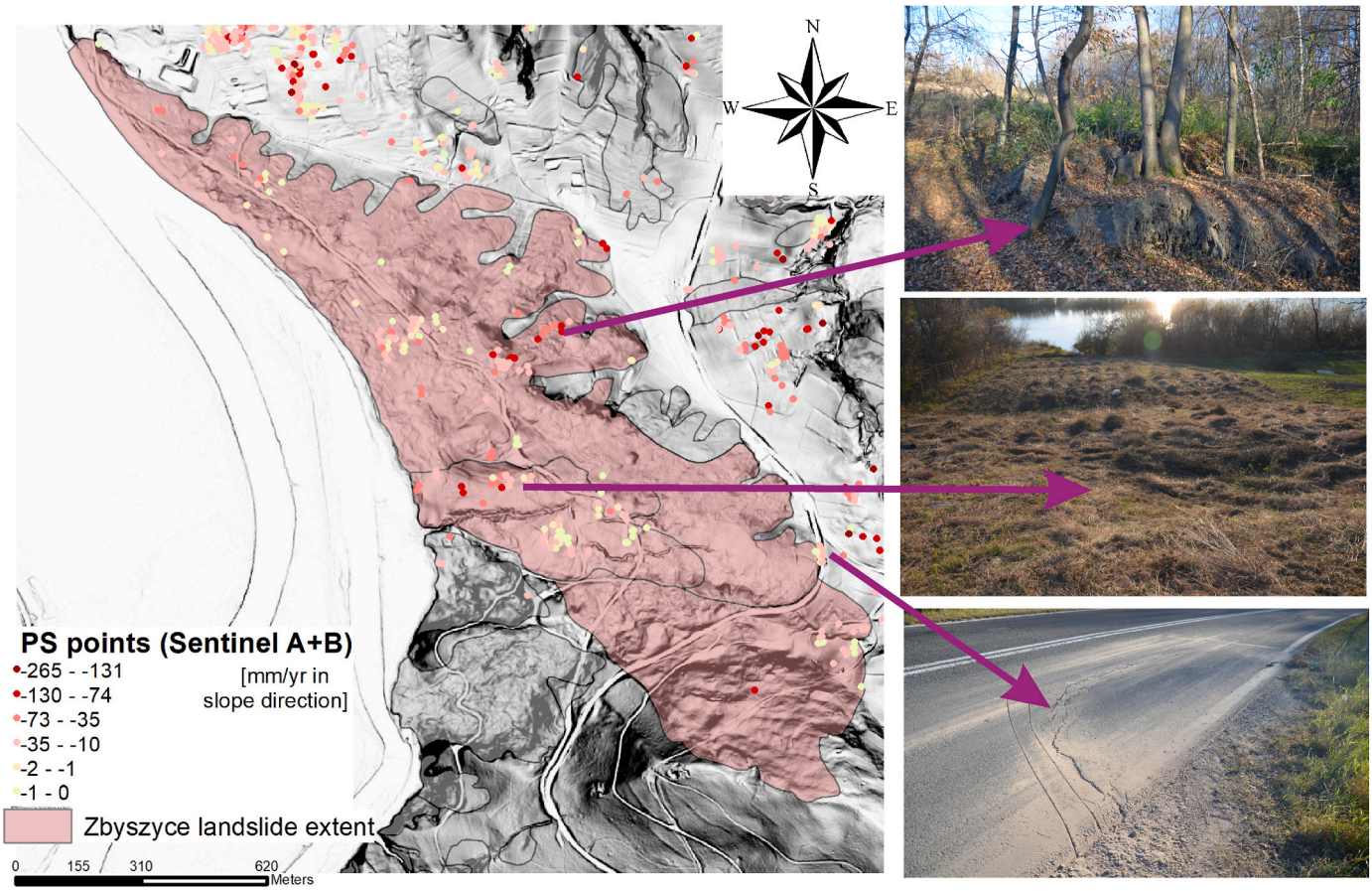

Fig. 12. Zbyszyce landslide activity evaluation during a field trip (photos taken on 03/07/2018).

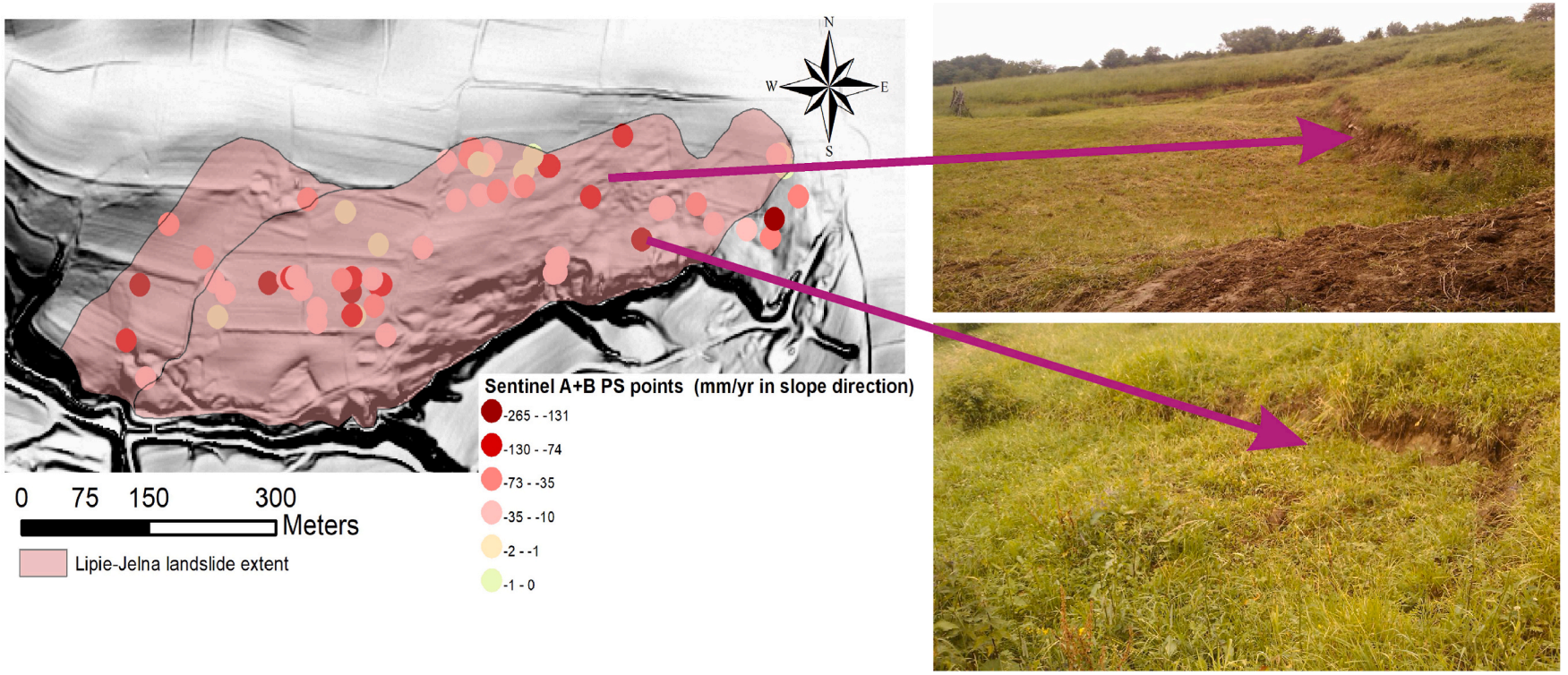

Fig. 13. Lipie-Jelna landslide activity evaluation during a field trip (photo taken on 03/07/2018).

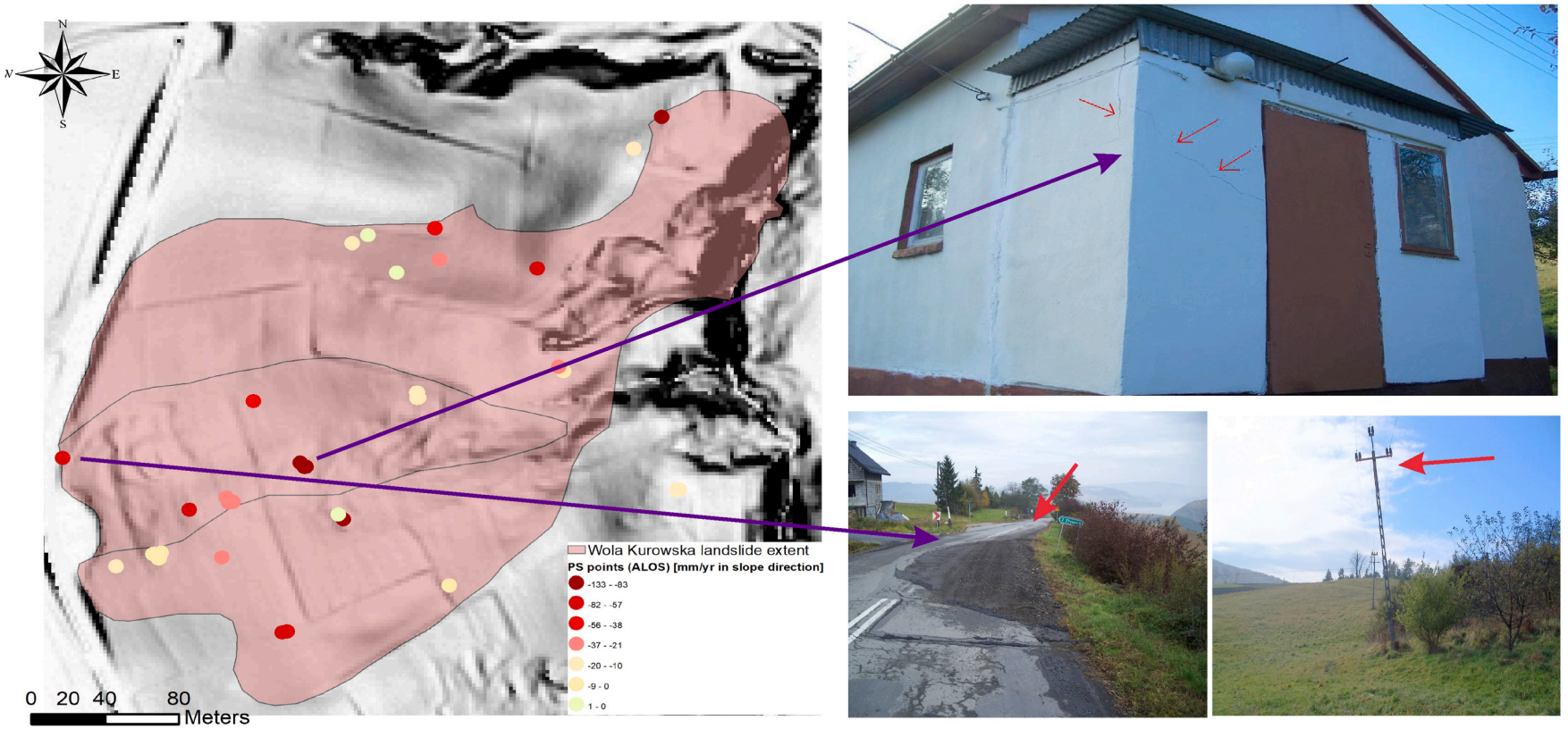

Fig. 14. Wola Kurowska landslide activity evaluation during a field trip (photo taken on 25/03/2011).

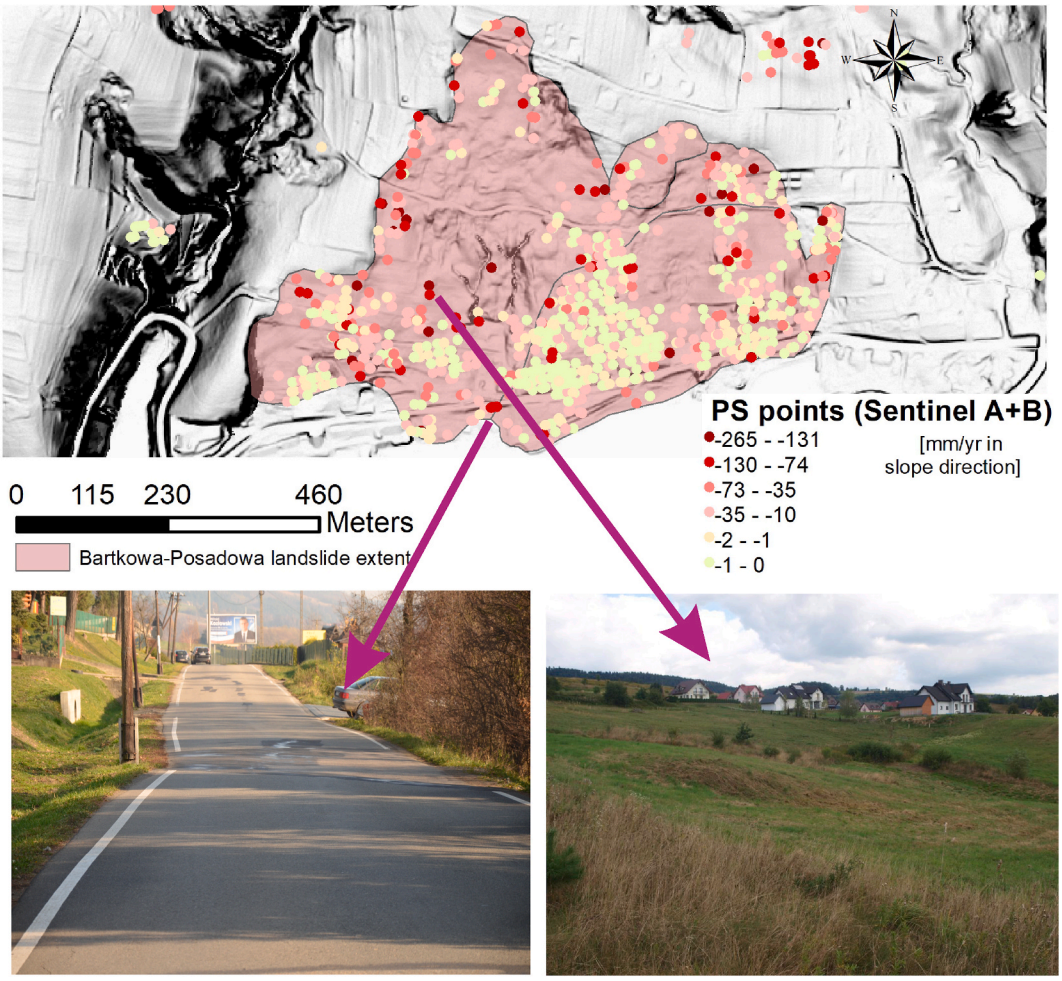

Fig. 15. Bartkowa-Posadowa landslide activity evaluation during a field trip (photos taken on 03/07/2018).

orbit modes. Moreover, many of the observed landslides have a sensitivity lower than one, which means that the real displacement rate can be much higher than that observed using interferometric techniques.

In summary, the PSInSAR analysis for both sensors, namely, ALOS PALSAR, and Sentinel images, reveals a quite satisfactory performance for assessing the landslide activity in the rural areas in the Polish Flysch Carpathians. ALOS PALSAR, thanks to the L-band sensor with a high penetration capacity, and Sentinel 1, thanks to its high temporal sampling (6 days), offer a great advantage in monitoring ground displacements. However, based on the abovementioned limitations connected with the underestimation of the displacement rates, it is recommended to evaluate the achieved results with in situ methods or field validation. These methods should be complementary to each other. The results retrieved by SAR interferometry can be considered as the initiation of the field inventory. Therefore, in this study, landslide activity states were evaluated by field reconnaissance. All landslides presented as examples of field verification, based on Mansour's thresholding, are expected to generate moderate damage to buildings and infrastructure. This fact was confirmed in the field, where the evidence of landslide activity was found by observing ground and infrastructure damage. In this context, the results of our investigations can leverage the application of the PSI approach in land use and land development studies. It can also support the reduction of urbanization pressures in the Rożnowskie Lake region mentioned by Kroh (2017).

5. Conclusions

In this research, landslide activities were studied based on PSInSAR analysis conducted on datasets delivered from three SAR-datasets, namely, ALOS PALSAR, Sentinel 1A, and Sentinel 1A/B. The landslide monitoring was carried out in the Polish Flysch Carpathians in the Małopolskie municipality, which has been widely affected by landslides for decades.

Landslide activity states and intensities were assessed based on the PSI-based matrix approach. The PSI analysis consisted of five diverse PSISAR processing for ALOS ascending mode, Sentinel ascending and descending modes (2014–2016), and for Sentinel ascending and descending modes (2017). Deformations in LOS direction were projected onto the steepest slopes. This allowed us to combine the ascending and descending results together as one PSI result. Additionally, for each PSInSAR result, potential damage maps were created based on the criteria of Mansour et al. (2011). Landslide activity states were also evaluated in situ. Some examples of field evaluation were presented together with general landslide characteristics.

In general, applying the PSI approach in rural areas is challenging. However, the results of this study prove that increasing the temporal sampling rate in view of launching the second Sentinel 1 satellite, provides a higher PS density and, therefore, this technique can deliver useful information for landslide activity assessment. PSInSAR processing of Sentinel 1A and Sentinel 1A/B allow to update activity state for 130 and 205 landslides, respectively.

From another point of view, the application of two Sentinel datasets from ascending and descending orbits, using only one Sentinel satellite (C band), allows us to achieve a similar PS density in comparison to the one ascending dataset of ALOS PALSAR (L-band). Overall, the outcomes of this work justify the potential of the PSI approach for landslide

activity and intensity assessment. We have shown that this technique can be beneficial for downstream applications related to landslides.

Availability of data and materials

Sentinel-1 data are freely available from Sentinel-Data-Hub website. Landslide data is also freely available on the website SOPO (http://geoportal.pgi.gov.pl/portal/page/portal/SOPO/Wyszukaj3).

Funding

The presented study was performed thanks to "START2020" scholarship founded by the Foundation for Polish Science and co-financed under the Leading Research Groups support project from the subsidy increased for the period 2020–2025 in the amount of 2% of the subsidy referred to Art. 387 (3) of the Law of 20 July 2018 on Higher Education and Science, obtained in 2019. The research infrastructure which has been used for computation purposes was created within the project EPOS-PL, European Plate Observing System POIR.04.02.00–14-A003/16, funded by the Operational Programme Smart Growth 2014–2020, Priority IV: Increasing the research potential, Action 4.2: Development of modern research infrastructure in the science sector, and co-financed by European Regional Development Fund.

Authors' contributions

Kamila Pawluszek-Filipiak performed the analysis of SAR images and preparation of the manuscript. Mahdi Motagh and Andrzej Borkowski contributed to design and supervised the experiment, contributed to writing, and revised the manuscript. All authors read and approved the final manuscript.

Declaration of competing interest

The authors declare that they have no known competing financial interests or personal relationships that could have appeared to influence the work reported in this paper.

Acknowledgements

The authors are very grateful to Tomasz Wojciechowski, Zbigniew Perski and Piotr Niescieruk for providing geological information, photographs, and documentation of the study area and for their support during field investigations accompanied by enlightening lectures. Furthermore, the authors are also grateful to the late Dr. Hans-Urlich Wetzelfor his valuable discussions connected with landslide geological issues. Anonymous reviewers also provided thoughtful and detailed comments that greatly improved the final version of this article. ALOS original data is copyright Japanese Aerospace Exploration Agency and provided under proposal ER2A2N189. Sentinel-1 data provided by ESA/Copernicus.

List of abbreviations

ALOS	Advanced Land Observing Satellite-1 (ALOS) PALSAR- Phased Array type L-band Synthetic Aperture Radar
SAR	Synthetic Aperture Radar
LOS	Line-Of-Sight
LIM	landslide inventory map
DInSAR	differential interferometry SAR
SBAS	Small BAseline Subset
PSI	Persistent Scatterers Interferometry
PSInSAR	Persistent Scatterer Interferometry (algorithm proposed by Ferretti et al., 2000,2001)
MTInSAR	multi-temporal interferometric techniques
ESA	European Space Agency
SOPO	The Landslide Counteracting System (pre-existing landslide inventory database)

Appendix B. Supplementary data

Supplementary data to this article can be found online at https://doi.org/10.1016/j.rsase.2021.100629.

Ethical Statement for Solid State Ionics

Hereby, I/insert author name/consciously assure that for the manuscript/insert title/the following is fulfilled:

1) This material is the authors' own original work, which has not been previously published elsewhere.
2) The paper is not currently being considered for publication elsewhere.
3) The paper reflects the authors' own research and analysis in a truthful and complete manner.
4) The paper properly credits the meaningful contributions of co-authors and co-researchers.
5) The results are appropriately placed in the context of prior and existing research.
6) All sources used are properly disclosed (correct citation). Literally copying of text must be indicated as such by using quotation marks and giving proper reference.
7) All authors have been personally and actively involved in substantial work leading to the paper, and will take public responsibility for its content.

The violation of the Ethical Statement rules may result in severe consequences.

To verify originality, your article may be checked by the originality detection software iThenticate. See also http://www.elsevier.com/editors/plagdetect.

I agree with the above statements and declare that this submission follows the policies of Solid State Ionics as outlined in the Guide for Authors and in the Ethical Statement.

References

Aslan, G., Foumelis, M., Raucoules, D., De Michele, M., Bernardie, S., Cakir, Z., 2020. Landslide mapping and monitoring using persistent scatterer interferometry (PSI) technique in the French alps. Rem. Sens. 12 (8), 1305.

Barra, A., Monserrat, O., Mazzanti, P., Esposito, C., Crosetto, M., Scarascia, Mugnozza, G., 2016. First insights on the potential of Sentinel-1 for landslides detection. Geomatics, Nat. Hazards Risk 7, 1874–1883. https://doi.org/10.1080/19475705.2016.1171258.

Béjar-Pizarro, M., Notti, D., Mateos, R.M., Ezquerro, P., Centolanza, G., Herrera, G., et al., 2017. Mapping vulnerable urban areas affected by slow-moving landslides using Sentinel-1 InSAR data. Rem. Sens. 9 (9), 876.

Berardino, P., Fornaro, G., Lanari, R., Sansosti, E., 2002. A new algorithm for surface deformation monitoring based on small baseline differential SAR interferograms. IEEE Trans. Geosci. Rem. Sens. 40 (11), 2375–2383. https://doi.org/10.1109/TGRS.2002.803792.

Bianchini, S., Cigna, F., Righini, G., Proietti, C., Casagli, N., 2012. Landslide hotspot mapping by means of persistent scatterer interferometry. Environmental Earth Sciences 67 (4), 1155–1172. https://doi.org/10.1007/s12665-012-1559-5.

Bianchini, S., Herrera, G., Mateos, R.M., Notti, D., Garcia, I., Mora, O., Moretti, S., 2013. Landslide activity maps generation by means of persistent scatterer interferometry. Rem. Sens. 5 (12), 6198–6222. https://doi.org/10.3390/rs5126198.

Bonì, R., Bordoni, M., Vivaldi, V., Troisi, C., Tararbra, M., Lanteri, L., et al., 2020. Assessment of the Sentinel-1 based ground motion data feasibility for large scale landslide monitoring. Landslides 17, 2287–2299.

Burtan, J., Cieszkowski, M., Ślaczka, A., Zuchiewicz, W., 1991. W. Szczegółowa Mapa Geologiczna Polski w skali 1:50000, arkusz Męcina (1018). Central. Arch. Geolog. PIG-PIB Warszawa [Detailed Geological Map of Poland in a scale of 1: 50000, Męcina sheet (no. 1018)] [in Polish].

Bąk, M., Długosz, M., Gorczyca, E., Kasina, Kozioł, T., Wrońska-Wałach, D., Wyderski, P., 2011. Mapa Osuwisk I Terenów Zagrożonych Ruchami Masowymi W Skali 1:10000, Gm. Łososina Dolna pow. nowosądecki, woj. małopolskie [Map of landslides and areas threatened by mass movements on a scale of 1: 10000 Łososina Dolna commune, Nowosądeckie county, Małpolskie municipality] [in Polish].

Cascini, L., Cuomo, S., Pastor, M., Sorbino, G., Piciullo, L., 2012. Modeling of propagation and entrainment phenomena for landslides of the flow type: the May 1998 case study. In: In Proc. of 11th Int. Symposium on Landslides: Landslides and Engineered Slopes, Banf, Canada June, pp. 3–8.

Cascini, L., Peduto, D., Pisciotta, G., Arena, L., Ferlisi, S., Fornaro, G., 2013. The combination of DInSAR and facility damage data for the updating of slow-moving landslide inventory maps at medium scale. Nat. Hazards Earth Syst. Sci. 13 (6), 1527. https://doi.org/10.5194/nhess-13-1527-2013.

Chowaniec, J., Wójcik, A., Mrozek, T., Rączkowski, W., Nescieruk, P., Perski, Z., Wojciechowski, T., Marciniec, P., Zimnal, Z., Granoszewski, W., 2012. Osuwiska W Województwie Małopolskim. Atlas–Przewodnik. Wydaw. Kartograf. Compass. ISBN, Kraków, pp. 978–983 ([Landslides in the Małopolskie voivodeship. Atlas-Guide] [in Polish]).

Cigna, F., Bianchini, S., Casagli, N., 2013. How to assess landslide activity and intensity with Persistent Scatterer Interferometry (PSI): the PSI-based matrix approach. Landslides 10 (3), 267–283. https://doi.org/10.1007/s10346-012-0335-7.

Crosetto, M., Biescas, E., Duro, J., Closa, J., Arnaud, A., 2008. Generation of advanced ERS and Envisat interferometric SAR products using the stable point network technique. Photogramm. Eng. Rem. Sens. 74 (4), 443–450. https://doi.org/10.14358/PERS.74.4.443.

Crosetto, M., Monserrat, O., Cuevas-González, M., Devanthéry, N., Crippa, B., 2016. Persistent scatterer interferometry: a review. ISPRS J. Photogrammetry Remote Sens. 115, 78–89. https://doi.org/10.1016/j.isprsjprs.2015.10.011.

Crozier, M.J., 1986. In: Landslides: Causes, Consequences Environment. Taylor Francis.

Cruden, D.M., Varnes, D.J., Turner, A.K., Schuster, R.L., 1996. Landslide types and processes. In: Landslides: Investigation and Mitigation, Special Report This Issue. 247. National Research Council. Transportation Research Board. National Academy of Science Press, Washington DC, pp. 36–75.

Del Ventisette, C., Righini, G., Moretti, S., Casagli, N., 2014. Multitemporal landslides inventory map updating using spaceborne SAR analysis. Int. J. Appl. Earth Obs. Geoinf. 30, 238–246. https://doi.org/10.1016/j.jag.2014.02.008.

Ferretti, A., Prati, C., Rocca, F., 2000. Nonlinear subsidence rate estimation using permanent scatterers in differential SAR interferometry. IEEE Trans. Geosci. Rem. Sens. 38 (5), 2202–2212. https://doi.org/10.1109/36.868878.

Ferretti, A., Prati, C., Rocca, F., 2001. Permanent scatterers in SAR interferometry. IEEE Trans. Geosci. Rem. Sens. 39 (1), 8–20. https://doi.org/10.1109/36.898661.

Ferretti, A., Fumagalli, A., Novali, F., Prati, C., Rocca, F., Rucci, A., 2011. A new algorithm for processing interferometric data-stacks: SqueeSAR. IEEE Trans. Geosci. Rem. Sens. 49 (9), 3460–3470. https://doi.org/10.1109/TGRS.2011.2124465.

Gorczyca, E., Wrońska-Wałach, D., Długosz, M., 2013. Landslide hazards in the polish flysch Carpathians: example of lososina dolna commune. In: Geomorphological Impacts of Extreme Weather. Springer, Dordrecht, pp. 237–250. https://doi.org/10.1007/978-94-007-6301-2_15.

Guzzetti, F., Mondini, A.C., Cardinali, M., Fiorucci, F., Santangelo, M., Chang, K.T., 2012. Landslide inventory maps: new tools for an old problem. Earth Sci. Rev. 112 (1–2), 42–66. https://doi.org/10.1016/j.earscirev.2012.02.001.

Haghshenas Haghighi, M., Motagh, M., 2016. Assessment of ground surface displacement in Taihape landslide, New Zealand, with C-and X-band SAR interferometry. N. Z. J. Geol. Geophys. 59 (1), 136–146. https://doi.org/10.1080/00288306.2015.1127824.

Herrera, G., Gutiérrez, F., García-Davalillo, J.C., Guerrero, J., Notti, D., Galve, J.P., et al., 2013. Multi-sensor advanced DInSAR monitoring of very slow landslides: the Tena Valley case study (Central Spanish Pyrenees). Rem. Sens. Environ. 128, 31–43. https://doi.org/10.1016/j.rse.2012.09.020.

Hooper, A., Zebker, H., Segall, P., Kampes, B., 2004. A new method for measuring deformation on volcanoes and other natural terrains using InSAR persistent scatterers. Geophys. Res. Lett. 31 (23) https://doi.org/10.1029/2004GL021737.

Kalia, A.C., 2018. Classification of landslide activity on a regional scale using persistent scatterer interferometry at the moselle valley (Germany). Rem. Sens. 10 (12) https://doi.org/10.3390/rs10121880, 1880. 1880.

Kampes, B.M., 2006. Radar Interferometry: Persistent Scatterer Technique. Springer, 2006.

Koluch, Z., Nowicka, D., 2012. Mapa Osuwisk I Terenów Zagrożonych Ruchami Masowymi W Skali 1:10000, Gm. Chełmiec, Pow. Nowosądecki, Woj małopolskie [Map of landslides and areas threatened by mass movements on a scale of 1: 10000 Chełmiec commune, Nowosądeckie county, Małpolskie municipality] [in Polish].

Kroh, P., 2017. Analysis of land use in landslide affected areas along the Łososina Dolna Commune, the Outer Carpathians, Poland. Geomatics, Nat. Hazards Risk 8, 863–875. https://doi.org/10.1080/19475705.2016.1271833.

Mansour, M.F., Morgenstern, N.R., Martin, C.D., 2011. Expected damage from displacement of slow-moving slides. Landslides 8 (1), 117–131. https://doi.org/10.1007/s10346-010-0227-7.

Meisina, C., Zucca, F., Notti, D., Colombo, A., Cucchi, A., Savio, G., et al., 2008. Geological interpretation of PSInSAR data at regional scale. Sensors 8 (11), 7469–7492. https://doi.org/10.3390/s8117469.

Meng, Q., Confuorto, P., Peng, Y., Raspini, F., Bianchini, S., Han, S., et al., 2020. Regional recognition and classification of active loess landslides using two-dimensional deformation derived from sentinel-1 interferometric radar data. Rem. Sens. 12 (10), 1541.

Monserrat, O., Crosetto, M., Devanthéry, N., Cuevas González, M., Barra, A., Crippa, B., 2016. Landslide inventory and monitoring using Sentinel-1 SAR imagery. In: Living Planet Symposium, vol. 740. European Space Agency, p. 308.

Motagh, M., Wetzel, H.U., Roessner, S., Kaufmann, H.A., 2013. TerraSAR-X InSAR study of landslides in southern Kyrgyzstan, central Asia. Remote sensing letters 4 (7), 657–666. https://doi.org/10.1080/2150704X.2013.782111.

Notti, D., Davalillo, J.C., Herrera, G., Mora, O., 2010. Assessment of the performance of X-band satellite radar data for landslide mapping and monitoring: upper Tena Valley case study. Nat. Hazards Earth Syst. Sci. 10 (9), 1865. https://doi.org/10.5194/nhess-10-1865-2010.

Notti, D., Herrera, G., ianchini, S., Meisina, C., García-Davalillo, J.C., Zucca, F., 2014. A methodology for improving landslide PSI data analysis. Int. J. Rem. Sens. 35 (6), 2186–2214. https://doi.org/10.1080/01431161.2014.889864.

Pawluszek, K., Borkowski, A., Tarolli, P., 2018. Sensitivity analysis of automatic landslide mapping: numerical experiments towards the best solution. Landslides 15 (9), 1851–1865. https://doi.org/10.1007/s10346-018-0986-0.

Perski, Z., Wójcik, A., 2010a. Karta Rejestracyjna Osuwiska (Numer Ewidencyjny 1210032-39020) W Miejscowości Zbyszyce [Landslide registration card along with an opinion no. 1210032-39020 in Zbyszyce] [in Polish].

Perski, Z., Wójcik, A., 2010b. Karta Rejestracyjna Osuwiska (Numer Ewidencyjny 12-10-032-20) W Miejscowości Wola Kurowska [Landslide Registration Card along with an Opinion in Wola Kurowska No. 12-10-032-20] [in Polish]).

Perski, Z., Hanssen, R., Wojcik, A., Wojciechowski, T., 2009. InSAR analyses of terrain deformation near the Wieliczka Salt Mine. Poland. Eng. Geolog. 106, 58–67. https://doi.org/10.1016/j.enggeo.2009.02.014.

Perski, Z., Wojciechowski, T., Borkowski, A., 2010. Persistent scatterer SAR interferometry applications on landslides in Carpathians (Southern Poland). Acta Geodyn. Geomater. 7 (3), 1–7.

Perski, Z., Borkowski, A., Wojciechowski, T., Wojcik, A., 2011. Application of persistent scatterers interferometry for landslide monitoring in the vicinity of Roznow Lake in Poland. Acta Geodyn. Geomater. 8 (3), 163, 2011.

Reyes-Carmona, C., Barra, A., Galve, J.P., Monserrat, O., Pérez-Peña, J.V., Mateos, R.M., et al., 2020. Sentinel-1 DInSAR for monitoring active landslides in critical infrastructures: the case of the rules reservoir (Southern Spain). Rem. Sens. 12 (5), 809.

Righini, G., Pancioli, V., Casagli, N., 2012. Updating landslide inventory maps using Persistent Scatterer Interferometry (PSI). Int. J. Rem. Sens. 33 (7), 2068–2096. https://doi.org/10.1080/01431161.2011.605087.

Rosi, A., Tofani, V., Tanteri, L., Stefanelli, C.T., Agostini, A., Catani, F., Casagli, N., 2018. The new landslide inventory of Tuscany (Italy) updated with PS-InSAR: geomorphological features and landslide distribution. Landslides 15 (1), 5–19. https://doi.org/10.1007/s10346-017-0861-4.

Sahraoui, O.H., Hassaine, B., Serief, C., Hasni, K., 2006. Radar interferometry with Sarscape software. Photogrammetry and Remote Sensing.

Shi, X., Zhang, L., Zhong, Y., Zhang, L., Liao, M., 2020. Detection and characterization of active slope deformations with Sentinel-1 InSAR analyses in the Southwest Area of Shanxi, China. Rem. Sens. 12 (3), 392.

Sousa, J.J., Hooper, A.J., Hanssen, R.F., Bastos, L.C., Ruiz, A.M., 2011. Persistent Scatterer InSAR: a comparison of methodologies based on a model of temporal deformation vs. spatial correlation selection criteria. Rem. Sens. Environ. 115 (10), 2652–2663. https://doi.org/10.1016/j.rse.2011.05.021.

Wasowski, J., Bovenga, F., 2014. Investigating landslides and unstable slopes with satellite Multi Temporal Interferometry: current issues and future perspectives. Eng. Geol. 174, 103–138. https://doi.org/10.1016/j.enggeo.2014.03.003.

Wojciechowski, T., Perski, Z., Wójcik, A., 2008. The use of satellite radar interferometry for the study of landslides in the Polish part of Karpaty. Przeglad Geol. 56, 12.

Wojciechowski, T., Borkowski, A., Perski, Z., Wojcik, A., 2012. Airborne laser scanning data in a landslide study - an example of a landslide in Zbyszyce (Outhern Carpathians). Przeglad Geol. 60, 95–102.

Wójcik, A., Krawczyk, M., 2010. Karta Rejestracyjna Osuwiska (Numer Ewidencyjny 12-40-032-38 W Miejscowości Lipie-Jelna [Landslide registration card along with an opinion no. 12-40-032-38 in Lipie Jelna] [in Polish].

Wójcik, A., Nowicka-Gorczyca, D.E., Wrońska-Wałach, D., 2011. Karta Rejestracyjna Osuwiska (Numer Ewidencyjny 1210102-23374) W Miejscowości Wieliczka [Landslide registration cart along with an opinion in Wieliczka no. 1210102-23374] [in Polish].

Wójcik, A., Wojciechowski, T., Wódka, M., Krzysiek, U., 2015. Objaśnienia Do Mapy Osuwisk I Terenów Zagrożonych Ruchami Masowymi W Skali 1:10000, Gm. Gródek Nad Dunajcem pow. nowosądecki, woj. Małopolskie [Explanations for the map of landslides and areas threatened by mass movements on a scale of 1: 10000 Gródek nad Dunajcem commune, Nowosądeckie county, Małpolskie manucipality] [in Polish].

WP/WLI, 1993. In: Working Party on World Landslide Inventory Multilingual Glossary for Landslides," the Canadian Geotechnical Society. BiTech Publisher, Richmond.

Zhou, C., Cao, Y., Yin, K., Wang, Y., Shi, X., Catani, F., Ahmed, B., 2020. Landslide characterization applying Sentinel-1 images and InSAR technique: the Muyubao landslide in the three gorges reservoir area, China. Rem. Sens. 12 (20), 3385.